
# Under Pressure: A Laboratory Investigation into the Effects of Mechanical Loading on Charred Organic Matter in Archaeological Sites



Citation for the original published paper (version of record):

Ngan-Tillard, D., Dijkstra, J., Verwaal, W. et al (2015). Under Pressure: A Laboratory Investigation into the Effects of Mechanical Loading on Charred
Organic Matter in Archaeological Sites. Conservation and Management of Archaeological Sites, 17(2): 122-142. http://dx.doi.org/10.1080/13505033.2015.1124179

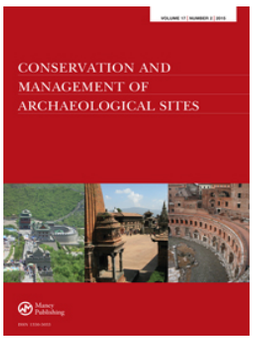

Routledge
Taylor & Francis Group

Conservation and Management of Archaeological Sites

ISSN: 1350-5033 (Print) 1753-5522 (Online) Journal homepage: https://www.tandfonline.com/loi/ycma20

# Under Pressure: A Laboratory Investigation into the Effects of Mechanical Loading on Charred Organic Matter in Archaeological Sites

**Dominique Ngan-Tillard, Jelke Dijkstra, Wim Verwaal, Arno Mulder, Hans (D.J.) Huisman & Axel Müller**

**To cite this article:** Dominique Ngan-Tillard, Jelke Dijkstra, Wim Verwaal, Arno Mulder, Hans (D.J.) Huisman & Axel Müller (2015) Under Pressure: A Laboratory Investigation into the Effects of Mechanical Loading on Charred Organic Matter in Archaeological Sites, Conservation and Management of Archaeological Sites, 17:2, 122-142, DOI: 10.1080/13505033.2015.1124179

**To link to this article:** https://doi.org/10.1080/13505033.2015.1124179



Published online: 08 Jan 2016.

CONSERVATION AND MGMT OF ARCH. SITES, Vol. 17 No. 2, May 2015, 122–142

# Under Pressure: A Laboratory Investigation into the Effects of Mechanical Loading on Charred Organic Matter in Archaeological Sites

DOMINIQUE NGAN-TILLARD,[1] JELKE DIJKSTRA,[2] WIM VERWAAL,[1] ARNO MULDER,[1] HANS (D.J.) HUISMAN,[3,4] and AXEL MÜLLER[5]

[1] *Delft University of Technology, The Netherlands*
[2] *Chalmers University of Technology, Gothenburg, Sweden*
[3] *Cultural Heritage Agency of the Netherlands, The Netherlands*
[4] *Leiden University, The Netherlands;* [5] *ADC Archeologie, Amersfoort, The Netherlands*

The present publication investigates what happens to archaeological sites when they are built over. Focus is put on the degradation of charred organic materials by static loading. It is assumed that materials lose archaeological value if their fragments become too small to be recovered, or too distorted to be classified at species level. Several charred ecofacts of a few millimetres in size (wood fragments, hazelnut shells, and seeds) have been selected and subjected to individual particle strength tests. Assemblages of these particles have also been compressed one-dimensionally and scanned at several stages of testing using laboratory based X-ray microtomography. Microscopic damage by splitting or crushing is found to be limited at the macroscopic yield stress. It initiated at stresses less than 80 kPa for the weakest assemblages, and in all cases at stresses below 320 kPa. (80 kPa represents the load of a 6 m high sand embankment on soft soil that has half-settled underneath the groundwater table, while 320 kPa corresponds to stresses applied beneath the pile foundation level of high-rise buildings.) Sand seeded with charred particles has also been tested to illustrate the beneficial effect of embedment of charred particles in sand during static one dimensional loading.

KEYWORDS charred organic matter, mechanical loading, one-dimensional compression, damage, X-ray microtomography

DOI 10.1179/1350503315Z.000000000106

## Introduction

### *Research context*

Archaeological remains are increasingly considered to be valuable; as a link to the past, as a part of cultural heritage, and as a source for scientific research. The Malta treaty of 1992 acknowledged this value, and obliged the EU countries that have signed the agreement to protect their archaeological remains *in situ* (i.e. in the soil). The signing of this treaty and its ratification has led to a major change in the way archaeological remains are treated in many European countries. Specifically, development plans must now be preceded by research to establish whether archaeological remains would be damaged by these plans. If damage is likely, there are two basic options: either the plans are adapted to enable preservation *in situ*, or the archaeological remains are excavated in a rescue excavation prior to construction. The decision is often hampered because the effects of development on archaeological sites are unknown. Then, archaeologists take the 'better safe than sorry' approach; sites are excavated and lost for future generations.

An overview of the present knowledge of the effects of construction on archaeological sites was recently published (Huisman, et al., 2011; Huisman, 2012). This overview highlighted major gaps in our understanding of the processes which occur during and after construction works on an archaeological site. At present there are no tools and too little knowledge to predict the extent of deformation of sites and damage to artefacts and other materials. This is especially the case in line infrastructure developments (roads and railways), where soft soils like peats and clays are directly loaded by the super structure. Soft soils are notorious for their heterogeneity and high compressibility which render them prone to large (differential) settlements and lateral deformation, when they are mechanically loaded. The construction of a railway track or a road on soft soils often requires sand embankments that are from 1 m to more than 15 m high (the latter at crossings with other lines). Such embankments cause an increase in vertical stress ranging from a few kPa to more than 250 kPa. Part of the embankment sand is forced to penetrate into the subsoil and pushes it sideways. The largest threats to archaeological sites buried beneath a sand embankment are thought to be: i) the destruction of specific types of vulnerable artefacts or ecofacts embedded in heterogeneous and deformable soils, ii) the loss of the relationship between remains and soil features, iii) the deformation of soil features and layers, hampering their interpretation, and, iv) the loss of stratigraphic information that would make it possible to separate out remains from different periods (Huisman, et al., 2011; Huisman, 2012).

### *Research objectives and methodology*

Our research project aims to produce knowledge and tools that predict the extent of deformation of archaeological sites in soft soils that become buried beneath line infrastructure. In the present publication, focus is on the first threat: damage to weak remains as a result of mechanical loading of archaeological sites. Charred organic remains are among the most friable, and little is known about their mechanical resistance. Single particle strength tests and one-dimensional compression tests on assemblages of charred particles and mixtures of charred particles and sand have been carried out to gain

insight into damage susceptibility at elevated stress levels (equivalent to embankment heights). In this study, particle damage is equated to loss of archaeological value. In order to assess damage as a function of applied stress levels, the traditional analysis of the mechanical response of single particles and assemblages of particles is complemented with micro-CT tomography observations. Available knowledge acquired on the micromechanics of granular soils is used to interpret and generalize test results.

## Test procedures and results

### *Materials tested*

Charred materials are chemically very stable, especially in acidic soils, and can remain intact for long periods of time. Their study by archaeobotanists provides a wealth of information on food, food economy, ecology, and landscape management in the past. We used artificially created as well as archeologically recovered, charred seeds, fruit, and wood fragments of millimetre size (2 to 5 mm) for our investigation.

For the tests with artificially created material, we selected Emmer wheat grains charred in the controlled environment of a laboratory to different degrees of carbonization. This material represents charred cereal grains found at archaeological sites. Subsequently, we tested charred barley and oat grains, recovered from a thirteenth-century funerary urn in Deventer, The Netherlands. Finally, we used small pieces of wood charcoal and fragments of charred hazelnut shells that were recovered in large quantities from soil features from a Mesolithic river dune site at the intersection between the N23 national road and the Hanzen line railway in the municipality of Dronten, The Netherlands (Hamburg, et al., 2013).

Cereal grains have an oblong shape and are cut by a deep groove (crease) on one side. Modern wheat grains have uniform form and dimensions compared to medieval grains. The hazelnut shell fragments and the wood charcoals present different shapes: the first are curved; the second are parallelepiped and flaky. To highlight differences in degrees of carbonization, we used a Philips Environmental Scanning Electron Microscope (ESEM), to inspect the micro-structure of the particles at magnifications ranging from 100 to 1000 (Figure 1). Only the wheat grains charred at 370°C proved to be fully carbonized with complete fusion of their endosperm. They are also the most distorted. The medieval grains have been subjected to insufficiently high temperatures to chemically convert starch granules into gelatine. The darker hazelnut shells are crossed by pseudo-hexagonal shrinkage cracks.

In some mechanical tests, the charred particles were mixed with sand to various volume fractions. The fine aeolian sand (mean grain size 0.150 mm), from which the charcoals of the N23 excavation were extracted, was selected for these tests.

### *Individual particle strength tests*

#### Individual particle strength test procedure

A stiff loading frame was used to conduct displacement controlled (force measured) crushing tests on individual particles at a rate of 0.5–1 mm/min. Some particles were photographed before and after testing to illustrate the sustained damage. The wheat

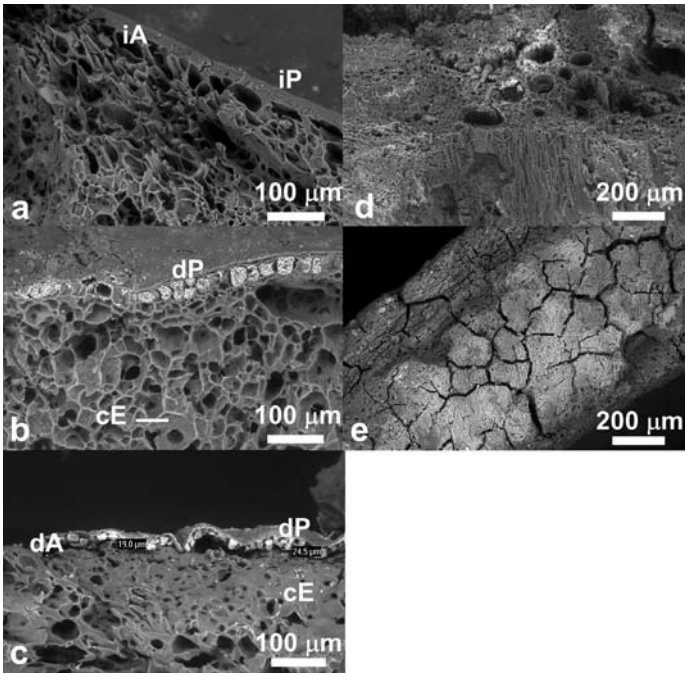


FIGURE 1 ESEM images of the charred materials. a: medieval grains, emmer wheat grains heated at b: 290°C and c: 370°C, d and e: charred materials from the N23 excavation in Dronten, d: wood charcoal, and e: charred hazelnut fragment. Note: in a–c, the intact (i) and distorted (d) pericarp (P) and aleurone layer (A), the converted endosperm (cE), and cavities of various size and wall thickness.

grains were placed either on their ventral position or their side position and loaded vertically between steel plates. The wood charcoals were loaded perpendicular to their longitudinal axis. The hazelnut fragments were loaded perpendicular to their curvature — the orientation with the largest chance of breakage under pressure.

## Results of individual particle strength tests

Very different behaviours were observed during the individual particle crushing tests. In brief: from very brittle, very stiff (hazelnut shells, Figure 2a), to very ductile (wheat grains heated to 370°C, Figure 2b), very compressible (wheat grains heated to 370°C, Figure 2b and wood charcoal, Figure 2c), with sudden splitting (hazelnut shells, Figure 2a), to progressive degradation before peak force (wheat grains heated to 270 and 290°C, Figure 2b and wood charcoal, Figure 2c). In some of the latter tests a clear peak force is not identified. The 370°C seeds could not bear more than 5 N. The hazelnut shells split at peak forces less than 10 N with a characteristic finger snapping sound. The wheat grains heated to 270°C and 290°C could bear 20 N on average before major splitting occurred. The wood charcoals were affected by asperity crushing and splitting along their fibres at only minor loading. However, it is often only after complete unloading that they fragment into multiple pieces, resulting in total loss of their archaeological value. The

undulations in their displacement-force curves are probably related to local failures, which were indistinguishable to the naked eye during loading. The medieval grains were found to be as weak as the grains charred at 370°C but responded more stiffly and in a more brittle manner (Figure 2b). Tests conducted on seeds parallel and perpendicular to the crease did not reveal any strength anisotropy. The thickest hazelnut shells and the largest charcoal pieces had the highest peak force. The complex irregular shape of

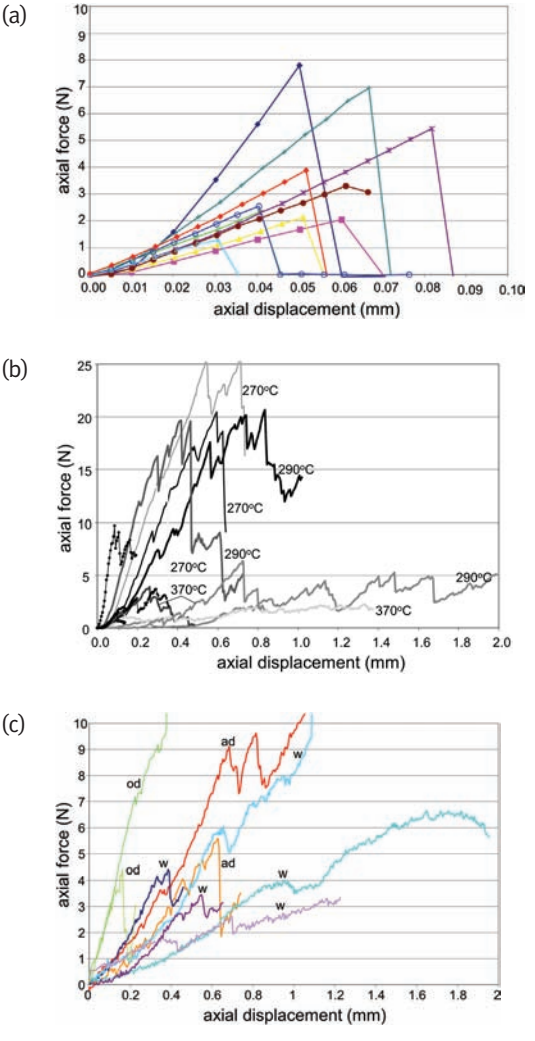


FIGURE 2 Typical behaviour observed during individual strength tests on a: hazelnut shell fragments, b: cereal grains, and c: wood charcoals. In 2b, red and yellow curves correspond to emmer wheat grains heated to 270°C, blue curves to emmer wheat grains heated to 290°C, green curves to emmer wheat grains heated to 370°C and black curves with black symbols to the medieval cereal grains. In 2c, thick reddish and yellowish curves are for air dried wood charcoals (ad), thick blue curves for wet wood charcoals (w), and thin curves for oven dried wood charcoals (od).

the particles prevented the conversion of the applied load and registered displacement into their respective normalized quantitates: stress and strain.

## *One-dimensional compression tests on assemblages of particles*

One dimensional compression tests (oedometer tests) were carried out on assemblages of charred particles to study their compressibility and yield characteristics in relation to the type and extent of damage sustained by the grains. The boundary conditions in these tests were selected to be a good representation for *in situ* loading conditions. The majority of the tests were performed on an assemblage of archaeological particles. In comparison to *in situ* conditions, where the particles are surrounded by soft soils; we expected larger stress concentrations from the lower number of particle contacts. As a result, a conservative estimate (i.e. worst case) for particle damage as function of vertical stress level is obtained.

### Conventional oedometer test procedure and interpretation in soil mechanics

In an oedometer test, a soil sample is compressed vertically while its lateral expansion is prevented (Figure 3a). During compression, the vertical stress is recorded or, vice versa, the vertical stress is imposed and the induced vertical compression recorded. The sample is fully confined so that it cannot fail macroscopically, but instead densifies. Densification can be associated to rearrangement and compression of the grains, which in turn can lead to microstructural damage.

Oedometric results are conventionally semi-logarithmically plotted in the void ratio vertical stress plane (e-log(σ)), the void ratio being the ratio between the volume of voids and the volume occupied by the solid material (Figure 3b). The change in void ratio (Δe) is related to the vertical strain (ε) as follows:

$$\Delta e = (1 + e_{\circ})\varepsilon \qquad (1)$$

where $e_{\circ}$ is the initial void ratio.

In the void ratio (or vertical strain) logarithm of the vertical stress plane, three phases of compression can be distinguished for a material made of uncemented, crushable grains (Figure 3b). At first, grains rearrange without breaking. Deformations are partly recoverable. Yield stress is the point of initiation of substantial particle damage in a granular material subjected to oedometric testing. Damage at the yield

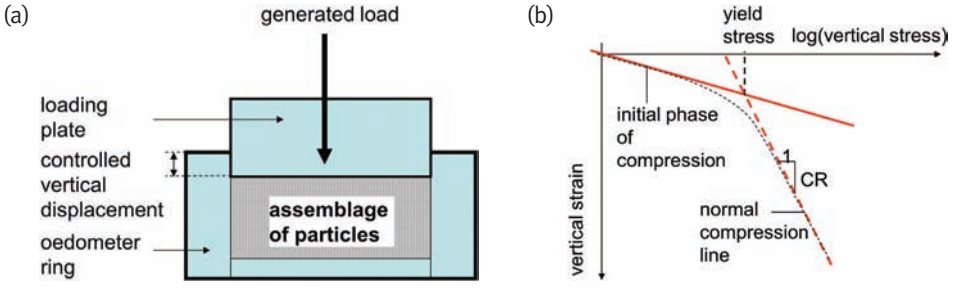


FIGURE 3 a: oedometer test apparatus and b: typical oedometer stress-strain curve.

stress is governed by grinding of the particle surface, asperity breakage at contact points between particles, and particle splitting (Nakata, et al., 2001). Geotechnical engineers pragmatically define yield stress as the highest curvature point of the vertical strain-logarithm of the vertical stress curve (Figure 3b). It is often indicated by the stress at the intersection point of the tangents to the first and third phases of compression. The third compression phase is referred to as the normal compression phase. It is reached after yielding —when the vertical strain is linearly correlated to the logarithm of the vertical stress. The slope of the linear section is defined as the compression ratio CR. In the third phase, damage is controlled by contact damage, continuous crushing of specific particles, breakage of particles which were still intact, and rearrangement of fragments. As broken pieces fill in voids, particles are fragmented into smaller and smaller pieces; the particle packing becomes stiffer with increasing stress.

## Oedometer testing combined with X-ray tomography

### *Test procedure*

In our experiments, we used an oedometer mould with an internal diameter of 60 mm, an external diameter of 70 mm, and a height of 30 mm. The mould was fabricated from a round polyether-ether-ketone (PEEK) bar. PEEK has a high stiffness and a high transparency for X-rays. It allows the imaging of the internal structure of a specimen inside its oedometer mould at different phases of loading by Micro-Computed X-ray tomography. In a micro-CT scanner, a source of X-ray illuminates the object and a planar X-ray detector collects magnified projection images. The object is rotated, and at each rotation angle an image is recorded. The images are combined to reconstruct the object in 3D. The reconstructed object is represented in a 3D cubic grid in which each 3D grid elementary volume (a voxel) has a specific grey value. The grey value is a measure of the linear X-ray attenuation coefficient of the materials present in that voxel. It depends on the local density and the chemical element(s) present in the voxel, together with the incident photon energy. The reconstructed object can be cut along multiple cross-sections with arbitrary orientations in order to inspect its internal structure. Cross-sections can be processed to measure 3D micro-structural parameters such as porosity, grain size distribution, shape, and orientation. The micro-CT scanner works using the same method as medical scanners used in hospitals, but on a smaller scale and at a much higher resolution. Resolution decreases with increasing object size. In this study, a resolution of 35 to 70 micrometres was achieved for a 70 mm diameter object. Scans were recorded with a Nanotom manufactured by Phoenix and processed with the AVIZO Fire software. The technical performance of the Nanotom is presented in Zacher, et al. (2010), while several issues regarding the processing of micro-CT images are discussed in Tarplee, et al. (2011).

Specimens with a height of approximately 30 mm were utilized, with the height being a compromise between minimizing boundary effects and particle scale effects. A larger specimen height increases friction on the side walls but reduces scale effects from particle size. The tests were conducted at a vertical displacement rate of 0.1 mm/min on air dried pluviated samples using a stiff loading frame. Several loading and unloading loops were applied up to 80, 160, 320 kPa, and, in a few cases,

TABLE 1 Oedometer tests on packings of charred particles — characteristics of the packings

| Specimen | Particle shape and size [mm] from scans (%) | 3D porosity estimated | Stress path loops with scans (X) |
|---|---|---|---|
| Wood charcoal of the N23 excavation (C1) | parallepipedic and flaky 4 to 6 mm long | 40 medium intragrain porosity | 0-20-0-80-0(X)<br>0-160-0 (X)<br>0-320-0 (X)<br>0-520-0 (X) |
| Wood charcoal of the N23 excavation (C2) | parallepipedic and flaky 1 to 4 mm long | 37 medium intragrain porosity | 0-20-0-80-0 (X)<br>0-160-0 (X)<br>0-320-0 (X)<br>0-520- 0 (X) |
| Hazelnut shells of the N23 excavation | curved 0.8 to 1.5 mm thick, 1 to 4 mm long | 46 low intragrain porosity | 0-20-0-80-0 (X)<br>0-160-0 (X)<br>0-320-0 (X) |
| Medieval oat and barley grains | oblongue 3 to 6 mm long, length/width=3 | low intergrain porosity, high intragrain porosity | 0-40-0-80-0 (X)<br>0-160-0 (X)<br>0-320-0 (X)<br>0-520-0 (X) |
| Wheat seeds charred at 270-290°C (replica) | oblongue about 5 mm long length/width=1.5 | high inter- and intragrain porosity | 0-40-0 (X)<br>0-80-0 (X)<br>0-120-0 (X)<br>0-200-0 (X)<br>0-320-0 (X)<br>0-520-0 (X) |
| Wheat seeds charred at 370°C (replica) | oblongue distored about 5 mm long | very high inter- and intragrain porosity | 0-40-10-<br>80-20-120-<br>0-200-35-<br>320-0-520-0 (X) |

520 kPa. The loading was designed to represent conditions found in the field. 80 kPa is reached during the construction of a 6 m high sand embankment on soft soil that has half settled into soft soil below the groundwater table, while 320 kPa corresponds to stresses applied below the pile foundation level of high-rise buildings. After unloading and before being loaded again, some specimens were scanned in the PEEK mould with the help of a micro-CT scanner. We conducted oedometer tests on a loose and a dense packing of large and small wood charcoals (C1 and C2); a loose packing of hazelnut shell fragments; a dense packing of medieval oat and barley grains; and loose packings of wheat seeds charred at 270 to 290, and 370°C. Dense packings of wheat grains charred at 290°C were also compressed to check the test repeatability. The characteristics of the packings are summarized in Table 1.

### *Tests on assemblages of charred organic particles: macroscopic observations*

The oedometric stress-strain curves are displayed using the natural strain rather than the linear strain formulation. Natural strain ($\varepsilon$) is more appropriate to normalize and compare large deformations ($\varepsilon > 7\%$) than linear strain ($\varepsilon_{lin}$). The one dimensional natural and linear strains are calculated as follows from the oedometer tests:

$$\varepsilon = \int \frac{dh}{h} = \int \frac{h - h_o}{h} = -\ln(h / h_o) \qquad (2)$$

and

$$\varepsilon_{lin} = \frac{dh}{h_o} = \frac{h - h_o}{h_o} \tag{3}$$

with ho and h, the initial and current specimen heights.

The curves are presented using both a linear and a logarithmic stress axis (Figures 4 and 5). For the sake of clarity, the curves for the medieval grains and the wheat grains charred at 270°C and 290°C are not shown. The linear plot better shows that specimens present different levels of stiffness and that their stiffness increases during compression. The softest specimens are the 370°C wheat and the loose wood charcoal specimens. The thirteenth-century seeds and the dense wood charcoal specimens have an intermediate stiffness. The hazelnut shells and the 270°C and 290°C wheat grain specimens are the stiffest. The increase in stiffness with strain is remarkable for the 370°C wheat seeds and the wood charcoals. Most of these differences in material response are obfuscated when the stress data is plotted on the log scale. All samples look similar, with each giving, after an initial phase at low stress, some evidence of a yield stress and a linear section at higher stress levels. For the wood charcoals and the cereal grains, the slopes of the linear sections are parallel. Hence, their compression ratio (CR) is the same. Specimens with a linear section to the left of the log plot have a lower stiffness (see the linear plot). For the hazelnut shells, the test was only taken up to 320 kPa. No clear macroscopic yield point could be observed from the oedometer data. Oedometer tests have to be performed to high stress levels so that the slope of the tangent to the end of a void ratio-log (stress) plot is not an arbitrary value, and the yield stress can be defined objectively.

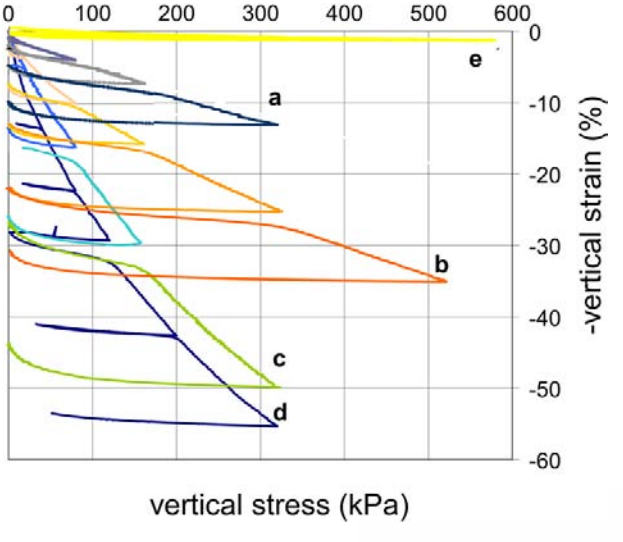


FIGURE 4 Oedometer stress-strain curves plotted with a linear stress axis, a: hazelnut shell fragments, b: wood charcoals, small particles, c: wood charcoal, larger particles, larger porosity, d: emmer wheat grains charred at 370°C, and e: 3 layers of wood charcoal pieces embedded in sand.

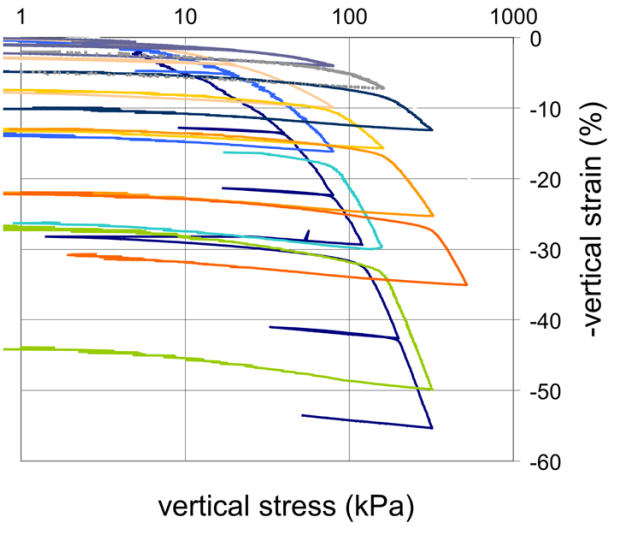


FIGURE 5 Same oedometer stress-strain curves as in Figure 4 plotted with a logarithmic stress axis.

The curvature of the yield phase is variable. It is the sharpest for the hazelnut shells and the most gentle for the 370°C charred wheat. The yield phase starts later for the hazelnut shells than for the wood charcoals, the lowest yield being associated to loose packings of large particles.

After loading — to any stress, and partial or full unloading— significant permanent deformation is observed. In the tests combined with scans, the specimens were systematically unloaded when the stress was twice as high as the stress before the previous unloading. The reloading curves, after complete unloading, converge slowly to the normal compression curve, in comparison to reloading curves after partial unloading. This indicates that complete unloading allowed some particle rearrangement.

Generally, our macroscopic observations follow the trends seen in the tests on individual particles. Assemblages of stiffer particles also respond more stiffly than assemblages of more compressible particles. However, the particulate level tenfold difference in initial stiffness between hazelnuts and charcoal is not observed for the assemblage. The latter only shows a twofold difference in initial stiffness.

### *Tests on assemblages of charred organic particles: microscopic observations*

There are major differences observed on the micro-CT scans in the mode of rearrangement and deformation of the grains. On one hand, under low stress, wood charcoal particles rearrange themselves without major breaking (Figures 6–8). The individual charcoals are compressible — they themselves become deformed. Once charcoal pieces have reached the locally tightest possible level of packing, particle damage occurs with further compaction. Grinding and plastic compression occur at contact points between particles. Small asperities break and particles indent into their neighbours. While grain

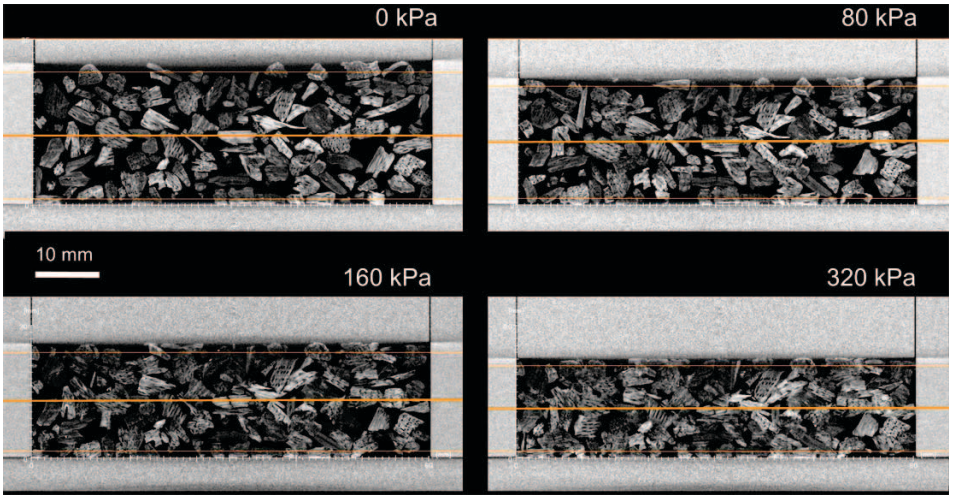


FIGURE 6 Assemblage of large wood charcoals with a high initial porosity at initial state and after loading to 80, 160, and 320 kPa. Vertical cross-sections. Note the high compressibility of the assemblage.

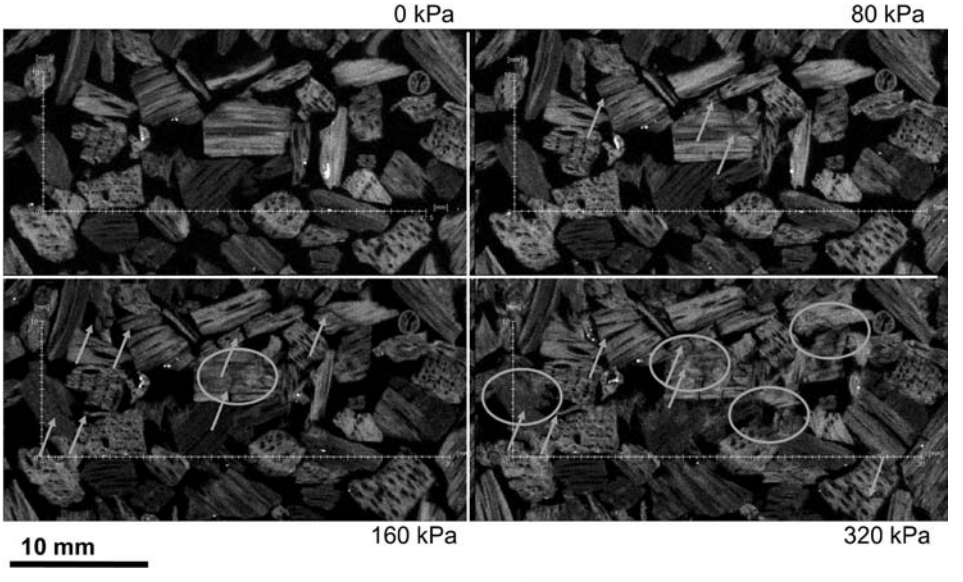


FIGURE 7 Zoom on the wood charcoals of the previous figure at the horizontal mid-section of the oedometer, at initial state, and after loading to 80, 160, and 320 kPa. Arrows point to cracks and ellipses highlight crushed zones. Damage is visible on the 80 kPa scan and is significant after 160 kPa loading.

indentation is discernible on the micro-CT scans, the finest pieces generated by grinding cannot be resolved on the micro-CT scans with a 35 μm resolution. It is mainly in the loosest packings, when particles have point contacts with very few neighbours (low

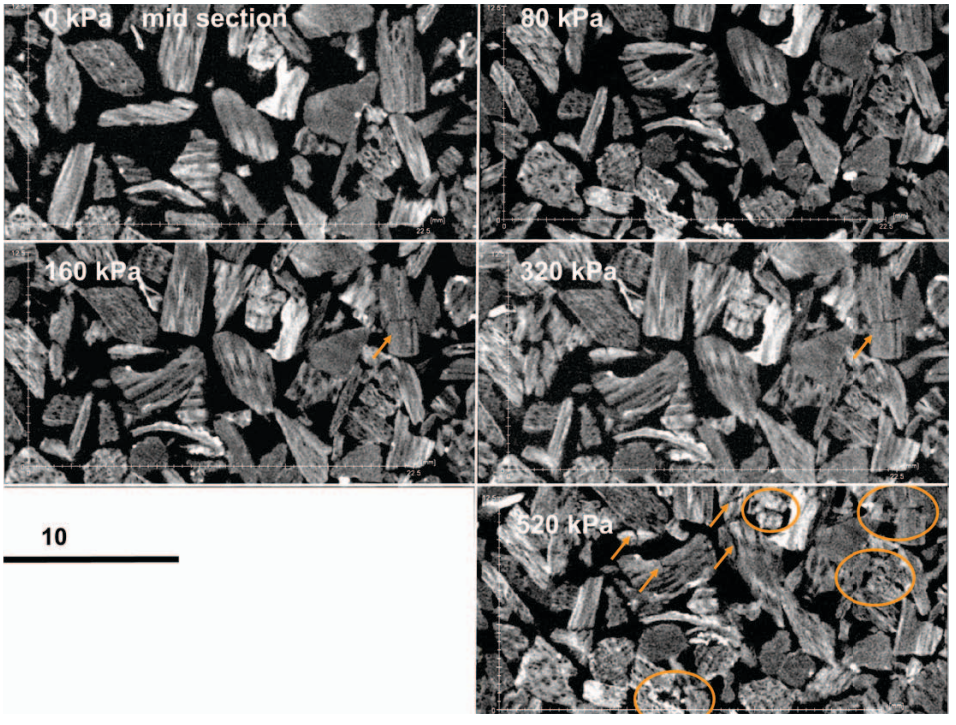


FIGURE 8 Assemblage of smaller wood charcoals with a lower initial porosity than those shown in figure 6. Zoom at the horizontal mid-section of the oedometer, at initial stage, and after loading to 80, 160, 320, and 520 kPa loading. Damage is not visible on the 80 kPa scan. The parallelepiped shape of the charcoals allows tangential contacts and mutual strengthening of adjacent grains to take place.

coordination numbers), that tensile splitting of particles is observed. At higher stresses, charcoal particles are forced to have more tangential contacts with their neighbours (the particles fuse); they are further compressed, and crumble into many pieces.

On the other hand, at the start of the test, curved hazelnuts shells are arranged in a loose packing. They have low grain compressibility, and, because of their shape, interlock and only slightly rearrange before further compaction causes failure in flexure into a limited number of pieces (Figure 9). The coordination number at the start of the test determines the damage in subsequent loading, i.e. the particles with the lowest number of inter-particle contacts sustain damage first. These observations corroborate the large stiffness and brittle failure mechanism of these shells as observed in the single particle tests. Fragmented hazelnut shells are not deformed internally and can easily be recognized with the naked eye. Archaeological loss is limited to small pieces that can pass through the mesh of coarse sieves.

The loosely packed 370°C wheat seeds are the weakest and the most compressible of all tested particles (Figure 10a). They fail gradually, which explains the low curvature of their loading curve in Figure 5. At high stresses (520 kPa), the 370°C grains have completely disintegrated and fused with neighbouring grains (Figure 10b). They

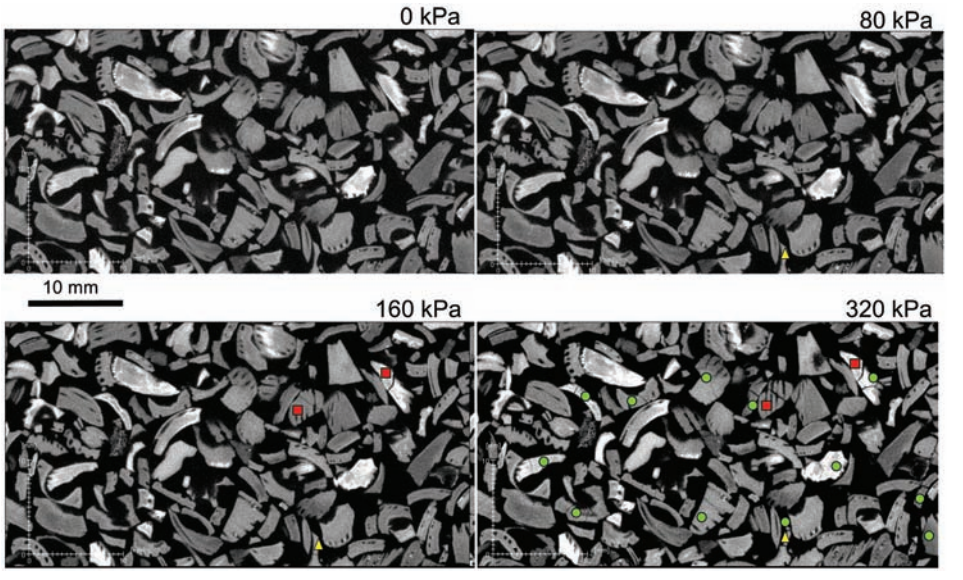


FIGURE 9 Assemblage of hazelnut shell fragments. Zoom at the horizontal mid-section of the oedometer, at initial state and after 80, 160, and 320 kPa loading. Limited damage occurs after 80 (triangles), and 160 kPa (squares) loadings. Damage is significant at 320 kPa (dots).

form a solid 'pancake' with extremely low intra- and intergranular porosity. Grains are so deformed internally that identification to species level by an archaeobotanist can be hampered.

The 270–290°C wheat grains are the strongest of all grains tested but not the most brittle. During loading, grain positions adjust so that the contact surface between grains increases. Contrary to the hazelnut fragments, the 270–290°C grains fail by

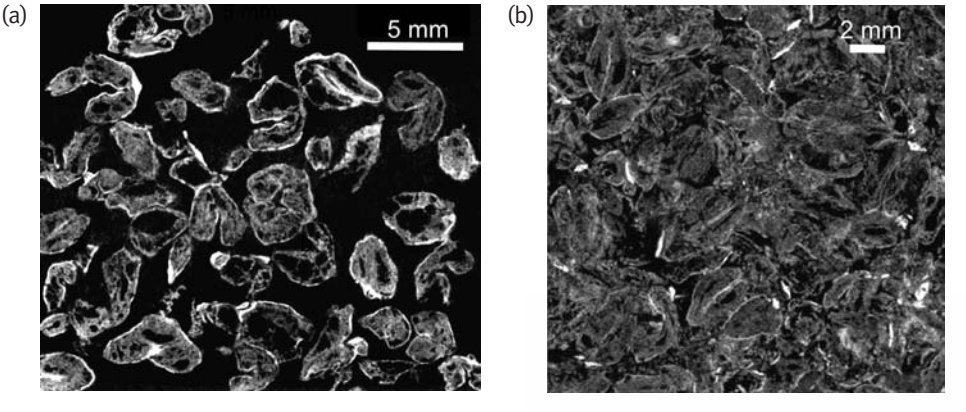


FIGURE 10 a: 370°C emmer wheat seeds before testing and, b: fused into a solid 'pancake' after 520 kPa loading, with an extremely low intra- and intergranular porosity.

internal crushing (Figure 11a). At 520 kPa, the intragranular porosity remains high (Figure 11b).

The medieval grains are almost as weak as the 370°C wheat grains, but they are brittle. With their wider spread grain size distribution, they formed an initial packing with a lower porosity (Figure 12). Despite their low particle strength, they yield at a higher stress.

On the micro-CT scans, deviations from the perfect sample and boundary conditions are highlighted. Obtaining a flat and homogeneous top surface with grains of millimetre size is particularly challenging. The contact of the top surface affects the first phase of the compression and therefore the determination of the yield stress. During testing, most damage occurred first at the top of the specimens, where the particles are in contact with a rigid boundary that constrains movement (Figure 13). Instead of adopting the classical determination of the yield stress (Figure 3b) we made a conservative estimation of the yield stress by reading the stress at the intersection of the virgin compression line with the horizontal axis at zero strain. This gave a yield stress of 55 to 135 kPa for more or less loose packings of wood charcoals and a minimum yield stress of about 70 kPa for the hazelnut shell fragments (Table 2). The first scans made above the yield stress show that visible damage at the middle of the sample is still very limited. Local grain damage by abrasion might have already taken place but cannot be discerned on the micro-CT scans. It can be thought that abrasion is not deteriorating the archaeological value of charred remains. Abraded grains have about the same size and can still be recovered by sieving and used for species identification. Crushing and tensile splitting results in fragmentation and therefore loss of archaeological value if particles become too small to be recovered. At 160 kPa about 2% of the hazelnuts, and 1% to 15% of the charcoal particles, depending on

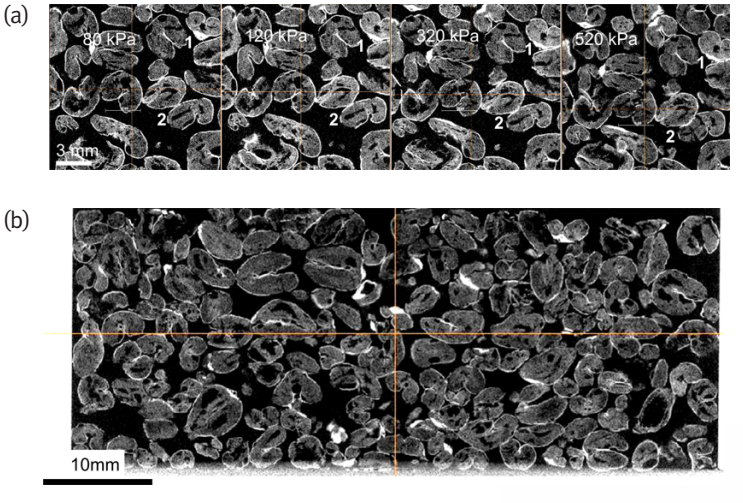


FIGURE 11 a: zoom on 290°C emmer wheat seeds during testing, from 80, to 120, 320 and 520 kPa. Note the formation of a tangential contact (label 1) and the step by step indentation of a grain (label 2); b: final packing at 520 kPa loading.

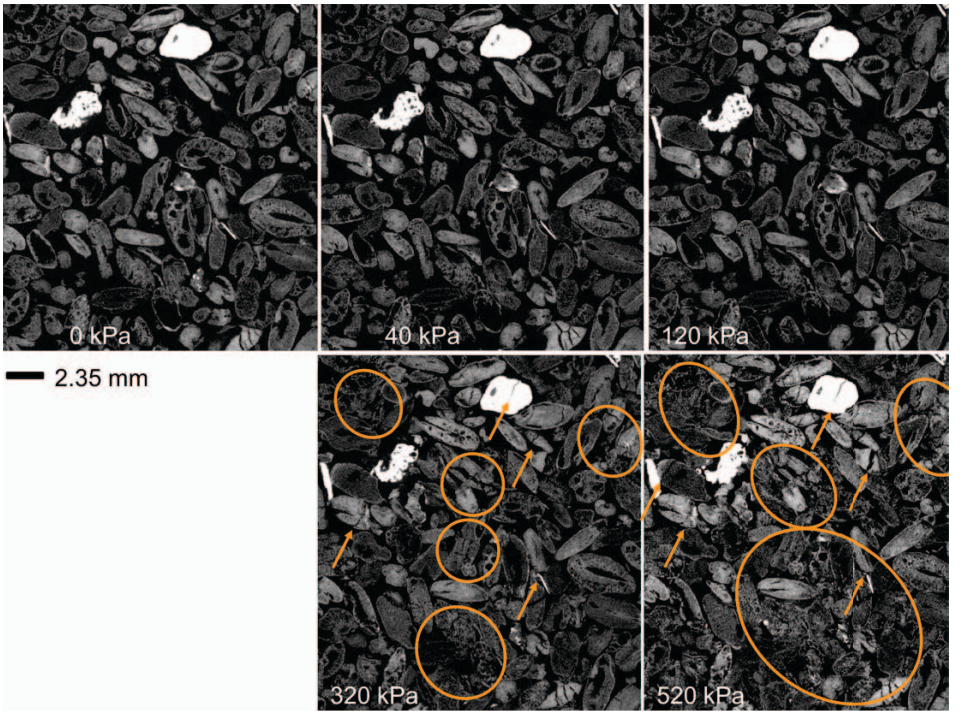


FIGURE 12 Medieval grains at the mid-horizontal section of the oedometer, at initial stage and after loading to 40, 120, 320 and 520 kPa. It is only on the scan at 320 kPa that damage is significant. Note the presence of more attenuating grains (in white) which are split on the 320 kPa scan.

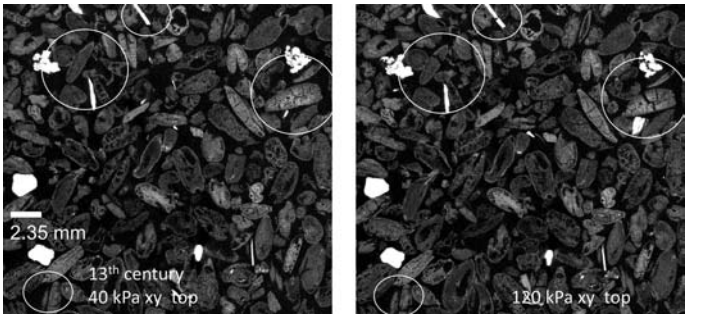


FIGURE 13 Medieval grains at the top horizontal section of the oedometer after 40 and 120 kPa loading. Several broken grains can be spotted on the scan made after 120 kPa.

the initial packing density, showed observable particle fractures in the centre of the specimen. Additionally, the charcoal particles showed large permanent particle re-arrangements and deformations. At 320 kPa, 10% of the hazelnut shell fragments, and about 20% to 80% of the wood charcoals, become damaged at the middle of the specimens.

TABLE 2 OEDOMETER TEST RESULTS

| Specimen | Yield stress [kPa] | Yield strain damage is visible at the middle of the specimen [%] | Loading at which damage is visible at the top of the specimen [kPa] | Loading at which [kPa] |
|---|---|---|---|---|
| C1 Wood charcoals | 54 | 11.8 | 80 | 80 |
| C2 Wood charcoal | 136 | 14.1 | 160 | 160 |
| Hazelnut shell fragments | > 67 | >3.9 | 160 | 80 |
| Medieval cereal grains | 119 | 10 | 320 | 120 |
| Wheat seeds charred at 270–290°C | 120 | 7.7 | | |
| Wheat seeds charred at 370°C | 43 | 14.4 | <<520 | <<520 |

### *Tests on charred particles embedded in sand*

Some tests were performed in the PEEK oedometer on samples of sand containing pieces of wood charcoal that had been arranged in different patterns. In one case, a few particles were spread at three different levels in the sand specimen. In another case, a layer of charcoal particles touching each other was formed and was either in direct contact with the sand or insulated from the sand by cling film. In all cases, the assemblage showed a very steep response (Figure 4). The charcoals were found to be undamaged except when placed in a layer insulated from the sand.

The sand samples seeded with charcoal pieces or with a layer of charcoal particles were also inspected after testing in a stiff brass oedometer ring up to very high stresses (1500 kPa). The charcoal pieces were found to be plastically undeformed. In such situations, rather than having contact points with neighbouring particles, the particles are supported by the surrounding sand. While subjected to stresses above 1500 kPa, they are not placed under tensile/flexural loading. Stress arching is also thought to have developed in the sand surrounding the soft charred particles; which protected them from high stress concentrations and eliminated the risk of local crushing. On the other hand, stiff particles embedded in a softer material (for example, hazelnut shell fragments in clay) attract stress. However, the stress concentration factor is lower than when particles are not supported by a (soft) matrix.

## Discussion

From research in soil mechanics, it is known that the yield stress, the curvature of the yielding phase in a $\varepsilon$-log($\sum$) plot, and the degree and type of particle damage, are dependent on particle characteristics (particle size, shape, roughness, tensile strength), and packing properties (void ratio, grain size distribution, coordination number, and heterogeneity of mineral composition). The yield stress reduces with a decrease of particle crushing strength (Golightly, 1990; McDowell & Bolton, 1998) and an increase of initial void ratio (Hagerty, et al., 1993; McDowell & Bolton, 1998; Nakata, et al., 2001), with packing uniformity and weak particle content in a

predominately strong-grained sand (Leleu & Valdes, 2007). The looser the packing, the higher the yield strain is. The yield stress is better defined for uniformly graded than for well-graded packings, and for packings made of brittle grains which break suddenly, rather than grains which fail gradually (Chuhan, et al., 2003; Leleu & Valdes, 2007). In well-graded packings, smaller grains sustain more splitting than larger grains (McDowell & Bolton, 1998; Nakata, et al., 2001; Muir Wood, 2007). Small grains have fewer neighbours than large grains, so they are subjected to larger stress concentrations close to those of the tensile splitting test, and break prematurely. Larger grains are confined by the forces acting at each of their (relatively numerous) contacts with neighbouring grains; they are affected by abrasion or asperity breakage rather than splitting. Note that this explanation only holds if the coordination number governs particle crushing more than the individual strength reduction with increasing particle size (McDowell & Bolton, 1998).

Most results on the role of particle crushing in the behaviour of soils have been obtained for quartz, feldspar, and carbonate sands. When loaded individually between two rigid platens, quartz grain fails suddenly, while feldspar and carbonate grains fail gradually: they experience a loss of bearing capacity when one of their asperities breaks and regains strength afterwards. Limited results are also available for gypsum. A gypsum grain can sustain large plastic deformation before failing. Its behaviour most resembles that of the wheat grains charred at 370°C, even if the wheat grain is characterized by a large inner porosity that collapses progressively during loading. The brittle behaviour of the quartz grains is the closest to that of the hazelnut shell fragments.

So far, most studies on the fate of particles during oedometric testing have been made using destructive techniques, in which the effects of stress could only be assessed *post mortem*. In some cases, materials were tested up to different stress levels and sieved after testing to quantify damage. Yamamuro, et al. (1996) made thin sections through unloaded samples for microscopic inspection. Cheng, et al. (2001) made live (non-destructive) observations of single particle behaviours through the glass loading plate of an oedometer at several stages of the same test. Their observations are limited to grains whose movements are restricted by a rigid boundary. We used micro-CT technology to observe the individual behaviour of carbonized seeds at several stages of the same compression test. Observations are three-dimensional. The charred particles present variable shapes, sizes, mechanical properties, and have an inner porosity. Hence, automatic particle segmentation for quantitative assessment of breakage, grain size distribution, and particle re-orientation is not trivial. Nevertheless the micro-CT scans are useful to understand the relationship between stress, strain, boundary conditions, damage type, and intensity in assemblages of archaeological remains. McBride & Mercer (2012) successfully exploited the same technology to detect damage in archaeological artefacts embedded in soil that had been repacked after one dimensional compression. They used a compression cell that was not transparent to X-rays. Scanning required specimen disassembly and did not allow observations at repeated or increased loads.

Our micro-CT observations give valuable insight into the behaviour of the sample. The kinematics of the particles within an assemblage corroborates the results on individual particles. The macroscopically obtained yield stress, and strain at yield, proved to be unreliable in assessing the particle damage within the assemblage. This is due

both to the difficulty in arriving at a yield stress, as well as the localized behaviour of damage within an assemblage.

Some limitations have been imposed on the test setup in order to allow for the novel examination of particle damage within the sample by means of micro-CT observations. Although the resulting scale and boundary effects caused by the relatively small number of grains in a specimen have influenced the test results, these have been conservative, i.e. more damage has been sustained in the tests when compared to *in situ*. The tests on sand with charcoal inclusions showed the beneficial effect that particle confinement, by sand, has on the preservation of charred particles during one dimensional loading.

In our investigation, specimens have been subjected to one dimensional compression that is representative of loading under the central part of an embankment. In such conditions, a soil densifies and cannot fail macroscopically with a loss of bearing capacity. In order to evaluate risk of macroscopic failure, any stress regime can be divided into mean stresses (equal normal stresses in all directions), and deviatoric stresses. The deviatoric stresses are the differences in normal stresses, and the shear stresses, that remain after subtracting the mean stresses from the stress regime. On one hand, assuming that the soil is isotropic, the dominant effect of an increase in mean stresses is a change of volume. The soil structure responds more stiffly, and as particles rearrange and eventually as pores and/ or particles get crushed, deforms permanently. On the other hand, deviatoric stresses are more disruptive than the corresponding levels of mean stresses. An increase in deviatoric stresses at constant mean stresses can lead to macroscopic failure with distortion and destruction of the soil structure. During one dimensional compression, the soil is primarily subjected to an increase in mean stresses and some increase in deviatoric stresses as horizontal stresses develop due to lateral restraint in proportion to (but not equal to) the vertical stress. As oedometric loading progresses, the mean stresses increase proportionally to the deviatoric stresses and the applied stress state deviates further from the compressive shear failure zone whilst it gets closer to the zone of permanent crushing deformation. Depending on packing and particle strength, crushing can occur from a certain mean stress level.

In some ground engineering applications, mean and deviatoric stresses develop in such a way that macroscopic compressive shear failure occurs. This can happen under foundation loads, at the toe of an embankment, the tip of a pile, or during excavation for the construction of an open pit or an underground space. Hyde (2004) and Hyde, et al. (2010) have already investigated the survival rate of archaeological inclusions of various shape, size, stiffness, and strength in sands undergoing changes in mean and deviatoric stresses up to macroscopic shear failure. They seeded triaxial sand samples with dyed particles that they studied for change of shape after testing. The particles were replicas of archaeological glass, ceramics, and bronze fragments. Test results have been incorporated into a probabilistic model for artefact survival with a certain degree of integrity. The probability of survival was found to be a function of the ratio of applied deviatoric stress to artefact flexural strength — the degree of integrity increasing, or remaining constant with increasing mean stresses. Micro-CT observations can be made at several stages of the loadings simulated by Hyde, et al. (2010) to gain insight into local modes of failure with respect to the development of diffuse or localized macroscopic failure patterns.

It should be noted that in any granular soils and especially in soils seeded with inclusions that are relatively soft or stiff, high deviatoric stresses with low mean stresses exist at particle level so that local distortion can take place, even under macroscopic oedometric conditions.

## Conclusion

X-ray microtomography has provided 3D evidence of damage in packings of charred organic particles subjected to oedometer tests as function of stress and strain. Loss of particle integrity has been observed for charcoals arranged in a loose packing at stresses that are applied during the construction of high sand embankments (5 m above ground surface or 6 m high with half of the embankment on soft soil settled under the groundwater table). Deformation modes varying from brittle tensile failure with limited particle rearrangement to grain crushing and indentation by neighbours, with large permanent intra- and intergrain deformation have been found to reflect the particle behaviour during individual crushing tests and their coordination number. Loss of archaeological value can be estimated from the micro-CT scans by calculating the percentage of particles fragmented into pieces that are too small to be retained on sieves and the percentage of particles that are so distorted that their identification to species level would be hindered.

In most common situations at archaeological sites, charred particles are embedded in soil. Undisturbed samples from archaeological sites can be subjected to our test procedure (oedometer test combined with X-ray micro-tomography). Next to oedometric loading, more destructive loadings (deviatoric, cyclic, and impact loadings) can be simulated. The stress level at which significant microscopic damage is observed in the laboratory can be used to determine whether or not loads applied during ground engineering works are likely to result in a loss of archaeological value. Archaeological soils containing various types of remains such as low-temperature fired ceramics, non-charred plant remains, fragile bones and shells, corroded metal coupons, etc., can be tested. The beneficial effect of embedment of charred particles in sand during static one-dimensional loading has already been proven. In future research, peaty and clayey soil types rich in ecofacts will be examined. Attention will be paid to the relative movement of archaeological inclusions with respect to their matrix, and loss of archaeological context will be investigated at microstructural level.

## Acknowledgements

We thank Otto Brinkkemper (Cultural Heritage Agency) for supplying us with medieval charred grains. The tests on prehistoric charcoal and charred hazelnut shells were done within the framework of the Hanze line railway project on the preservation of archaeological sites in Flevoland, funded by Prorail, subproject 2B.

## Bibliography

Cheng, Y.P., White, D.J., Bowman, E.T., Bolton, M.D., & Soga, K. 2001. The Observation of Soil Microstructure Under Load. In: Y. Kishino, ed. *4th International Conference on Micromechanics of Granular Media, Powders and Grains 2001, Sendai, Japan*. Rotterdam: A.A. Balkema Publishers, pp. 69–72.

Chuhan, F., Kjeldstad, A., Bjorlykke, K., & Hoeg, K. 2003. Experimental Compression of Loose Sands: Relevance to Porosity Reduction During Burial in Sedimentary Basins. *Canadian Geotechnical Journal*, 40(5): 995–1011.

Golightly, C.R., 1990. Engineering Properties of Carbonate Sands. PhD thesis, Bradford University.

Hagerty, M.M., Hite, D.R., Ullrich, C.R., & Hagerty, D.J. 1993. One-Dimensional High Pressure Compression of Granular Materials. *ASCE Journal of Geotechnical Engineering*, 119(1): 1–18.

Hamburg, T., Müller, A., & Quadvlieg, B. 2013. *Mesolithisch Swifterbant, Archol Rapport 174 en ADC rapport 3250*. Leiden: Archol BV.

Huisman, D.J., Bouwmeester, J., de Lange, G., van der Linden, Th., Mauro G., Ngan-Tillard, D.J.M., Groenendijk, M., de Ridder, T., van Rooijen, C., Roorda, I., Schmutzhart, D., & Stoevelaar, R. 2011. De invloed van bouwwerkzaamheden op archeologische vindplaatsen [online]. Rijksdienst voor het Cultureel Erfgoed [accessed February 2015]. Available at: <www.cultureelerfgoed.nl/bouwen-en-archeologie>.

Huisman, D.J. 2012. Deep Impact: What Happens when Archaeological Sites are Built Over? *Conservation and Management of Archaeological Sites*, 14(1–4): 60–71.

Hyde, A. 2004. Damage to Inclusions in Sand Subjected to One-Dimensional Compression. In: T. Nixon, ed. *Preserving Archaeological Remains In Situ? Proceedings of the 2nd Conference*. London: Museum of London Archaeology Service, pp. 32–39.

Hyde, A., Jackson, C.M., Hassan, I., & Howie, L.A. 2010. Probability of Damage to Archaeological Inclusions in a Sandy Matrix. In: M. Jiang, F. Liu, & M. Bolton, eds. *Geomechanics and Geotechnics, From Micro to Macro*. London: CRC Press, Taylor & Francis Group, pp. 253–57.

Leleu, S.L. & Valdes, J.R. 2007. Experimental Study of the Influence of Mineral Composition on Sand Crushing. *Géotechnique*, 57(3): 313–17.

McBride, R.A. & Mercer, G.D. 2012 Assessing Damage to Archaeological Artefacts in Compacted Soil using Microcomputed Tomography Scanning. *Archaeological Prospection*, 19: 7–19.

McDowell, G.R. & Bolton, M.D. 1998. On the Micromechanics of Cushable Aggregates. *Géotechnique*, 48(5): 667–79.

Muir Wood, D. 2007. The Magic of Sands, 20th Bjerrum Lecture: Oslo: November 2005. *Canadian Geotechnical Journal*, 44: 1329–50.

Nakata, Y., Hyde, A., & Murata, H. 2001. Microscopic Particle Crushing of sand Subjected to High Pressure One-Dimensional Compression. *Soils and Foundations*, 41(1): 69–82.

Tarplee, M.F.V., van der Meer, J.J.M., & Davis, G.R. 2011. The 3D Microscopic 'Signature' of Strain within Glacial Sediments Revealed using X-ray Computed Microtomography. *Quaternary Science Reviews*, 30: 3501–32.

Yamamuro, J.A., Bopp, P.A., Poul, V., & Lade, P.V. 1996. One-Dimensional Compression of Sands at High Pressures. *Journal of Geotechnical Engineering*, 122(2): 147–54.

Zacher, G., Santillan, J., Brunke, O., & Mayer, T. 2010. 3D Microanalysis of Geological Samples with High-Resolution Computed Tomography. In: K.A. Alshibli & A.H. Reed, eds. *Advances in Computed Tomography for Geomaterials*. London and Hoboken: ISTE & John Wiley, pp. 197–204.

## Notes on contributors

Jelke Dijkstra is Associate Professor at Chalmers University, Sweden, specialized in the micro-mechanics of geomaterials and physical modelling of foundations.

Wim Verwaal is a Technician at Delft University of Technology, an expert in microstructural investigation of natural and man-made materials using X-ray (micro-) tomography.

Arno Mulder is a Senior Technician at Delft University of Technology, expert in laboratory testing techniques for soils and rocks.

Hans (J.D.) Huisman is a Researcher in Soil Science and Degradation at the Cultural Heritage Agency of The Netherlands.

Axel Müller is a Senior Archaeologist at ADC ArcheoProjecten, specializing in ancient landscapes and the implementation of new techniques in archaeological research.

Dominique Ngan-Tillard is an Assistant Professor and an engineering geologist at Delft University of Technology, specializing in the degradation of geomaterials subjected to changing environments and on-site investigation in soft soils.

Correspondence to: Dominique Ngan-Tillard, TU Delft, CEG, PO Box 5048, 2600 GA Delft, The Netherlands. Email: d.j.m.ngan-tillard@tudelft.nl